Supporting information

Semi-metallic, Strong and Stretchable Wet-spun Conjugated Polymer Microfibers

Jian Zhou,[‖a] Er Qiang Li,[‖b] Ruipeng Li,[c] Xuezhu Xu, [d] Isaac Aguilar Ventura,[a] Ali Moussawi,[a] Dalaver H. Anjum,[e] Mohamed Nejib Hedhili,[e] Detlef-M. Smilgies,[c] Gilles Lubineau [*a] and Sigurdur T. Thoroddsen [*b]

This PDF file includes:

‖ Contributed equally to this work

[a] *King Abdullah University of Science and Technology (KAUST), Physical Sciences and Engineering Division, COHMAS Laboratory, Thuwal 23955-6900, Saudi Arabia; E-mail: gilles.lubineau@kaust.edu.sa; Tel:+966(12)8082983*

[b] *King Abdullah University of Science and Technology (KAUST), Physical Sciences and Engineering Division, High-Speed Fluids Imaging Laboratory, Thuwal 23955-6900, Saudi Arabia; E-mail: sigurdur.thoroddsen@kaust.edu.sa*

[c] *Cornell High Energy Synchrotron Source, Wilson Laboratory, Cornell University, Ithaca, New York 14853, USA.*

[d] *North Dakota State University, Department of Mechanical Engineering, Fargo, ND 58108, United States*

[e] *King Abdullah University of Science and Technology (KAUST), Advanced Nanofabrication, Imaging and Characterization Core Laboratory, Thuwal 23955-6900, Saudi Arabia*

1 Optimization of wet-spinning parameters

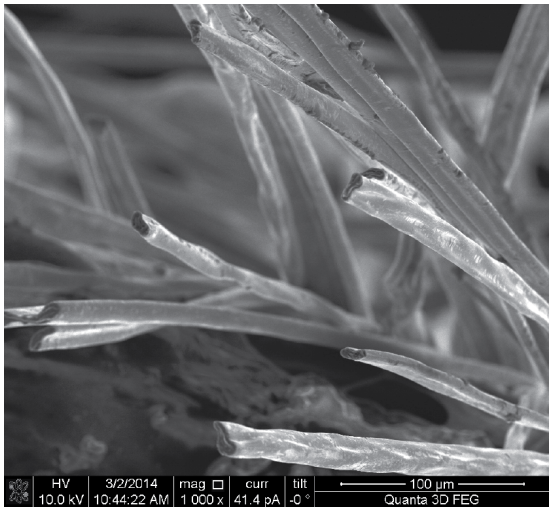

Fig. S1 SEM image showing irregular shapes of as-spun PEDOT/PSS microfibers without sufficient drying after winding to the drum collector.

Research has showed that fiber spinnability is greatly affected by various physical parameters, such as composition of the coagulation bath, the ink concentration and viscosity, the spinning speed and nozzle diameter.[1,2] Among these parameters, viscosity and spinning speed play the most important roles in obtaining continous fibers.

Spinning Dope Formulation Pristine PH1000 dispersion (11 mg/mL) can form fibers over a wide range of spin speeds from 0.3 to 150 μL/min. However, fibers can easily break in the coagulation bath or in the air due to the low viscosity of the dispersion. Higher concentrations of PH1000 dispersion (22 mg/mL) greatly improve the stability of the wet-spinning process due to the easier entanglement of the polymer chains. To improve the conductivity of the fibers, EG was mixed with the PH1000 dispersion (22 mg/mL) (this process was called EG doping). We found that 3 wt% of EG was the optimised concentration for doping concentrated PH1000 dispersion (22 mg/ml), and the final conductivity was as high as 607.0 $\pm$60.2 S/cm.

Fiber hot-drawing

After the "wet" fiber was taken from the coagulation bath, it was immediately heated and subjected to a vertical drawing process, as shown in Fig. 1b. The temperature around the fiber was controlled by two hot plates and monitored by a thermal couple. The draw ratio was calculated from the fiber collection speed and the wet-spinning speed. Fibers collected without hot drawing and with a draw ratio of 3.0 were first investigated. The distance between the collector and the surface of the coagulation bath was fixed at 50 cm to ensure that the fibers were dried before collecting on the rotating spool. Insufficient drying resulted in non-circular fibers on the collector, as shown in Fig. S1. The effect of hot-drawing on fiber conductivity is shown in Fig. S2.

Cogulation bath

By fixing the dispersion concentration at 22 mg/ml, and keeping the same collection speed, two kinds of coagulation baths were tried. Conductivity of the fibers was 231 $\pm$ 12 S/cm from the acetone bath, while the conductivity increased to 368$\pm$34 S/cm by using an acetone/IPA (volume ratio 1:1) bath. Research has shown that the conductivity of PEDOT/PSS films can be enhanced from 0.30 to 468 S/cm by IPA dip-

treatment for 10 min.[4] As the continuous wet-spinning process ends up with a dip time of 10 s for the fibers in the bath, the conductivity enhancement should be minimal. However, introducing IPA could greatly reduce the number of pores inside the fibers, which would result in better mechanical properties.[5,6]. Thus, in this study, a mixture of acetone/IPA (volume ratio 1:1) was used as the cogulation bath to maximized the fiber quality.

Spinnability Spinnability of the inks was monitored in an acetone/IPA (volume ratio 1:1) tank by a high speed camera. Commercial Clevios PH1000 ink after homogenization and sonication was first spun through a 50 μm glass nozzle. The concentration of prepared PH1000 ink (11 mg/mL) was relatively smaller compared with earlier studies, e.g., Clevios P (13 mg/mL), PH500 (11 mg/mL) and even Orgacon dry inks (15-30 mg/mL).[5,7,8] It is noted that PH1000 ink in the current study had a wide range of spin speeds from 0.3 to 150 μL/min.

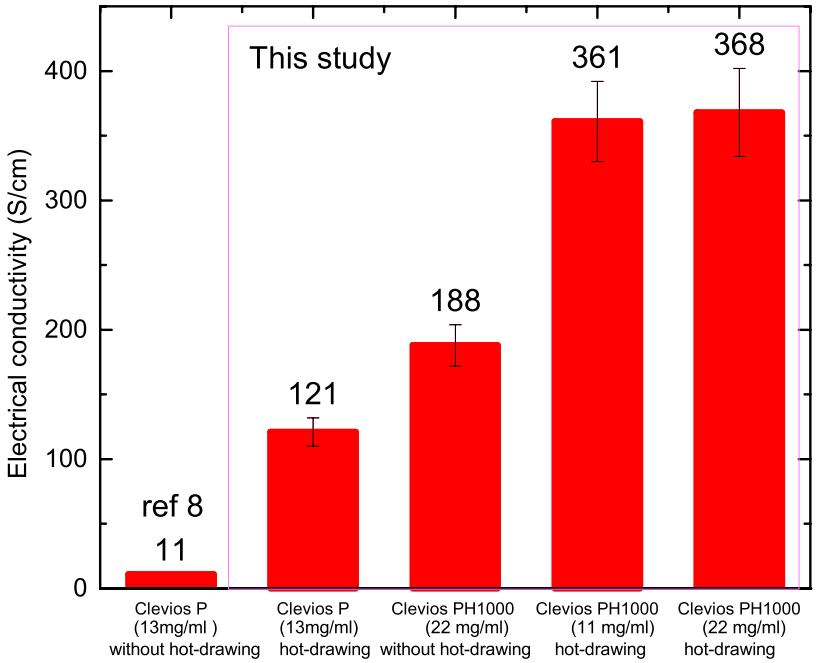

Fig. S2 The effect of hot-drawing on the conductivity of the fibers. The draw ratio was controlled to 3.0. The molecular weight of Clevios P is less than that of Clevios PH1000.[3]

Table S1 Summary of the electrical conductivity of EG doped and/or de-doped PEDOT/PSS fibers prepared from concentrated Clevios PH1000 (22 mg ml $^{-1}$).

Doped and/or de-doped PEDOT/PSS fiber type	Diameter (μm)	Conductivity (S cm^{-1})
EG/(PEDOT/PSS) fiber	9.7±1.4	607±60
(PEDOT/PSS)/EG fiber	8.6±0.8	1304±56
EG/(PEDOT/PSS)/EG fiber	8.4±0.7	2804±311

2 Morphology of conductive polymer fibers (SEM, AFM)

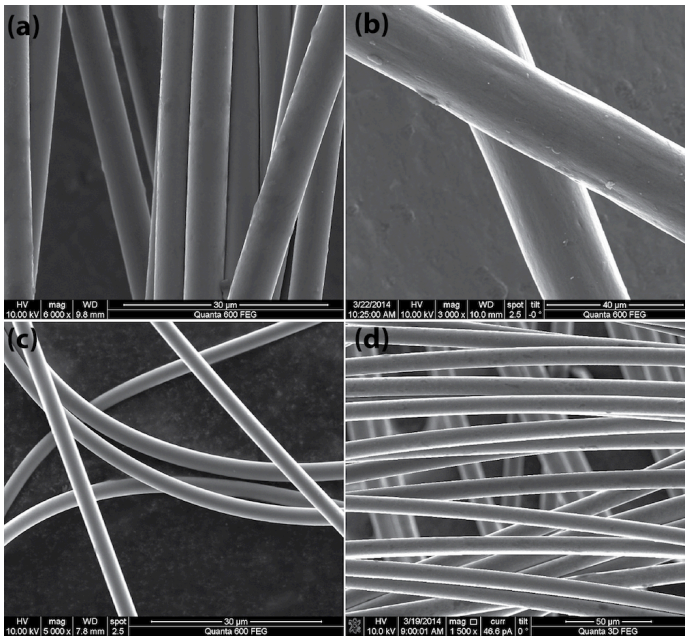

Fig. S3 SEM images of the conductive polymer microfibers. (a) PEDOT/PSS fibers spun from the 11 mg/mL dispersion with hot-drawing, (b) PEDOT/PSS fibers spun from the 22 mg/mL dispersion without hot-drawing (c) PEDOT/PSS fibers from the Clevios P dispersion (13 mg/ml). (d) 3 wt% EG doped PEDOT/PSS (EG/(PEDOT/PSS)) fibers spun from the 22 mg/mL dispersion. (a), (b) and (d) are spun from the Clevios PH1000 dispersion, (c) is spun from the Clevios P dispersion.

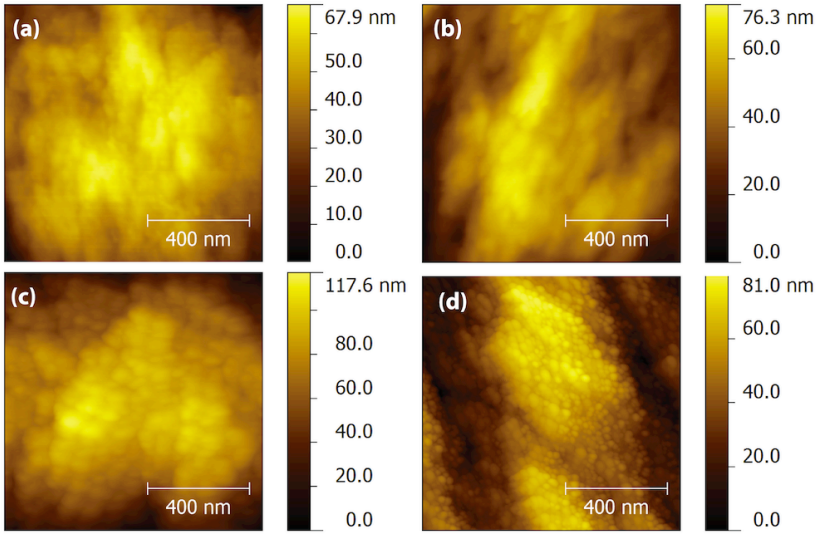

Fig. S4 AFM height images of the conductive polymer microfibers. (a) As-spun PEDOT/PSS fiber, (b) EG/(PEDOT/PSS) fiber, (c) (PEDOT/PSS)/EG fiber and (d) EG/(PEDOT/PSS/EG) fiber. All the images are 1 μm $\times$ 1 μm. Root to square (rms) roughness measured from these images are 11.2, 14.1, 21.8 and 18.0 nm for (a), (b), (c) and (d) respectively.

3 Microstructure characterization (XRD and Raman) of PEDOT/PSS fibers

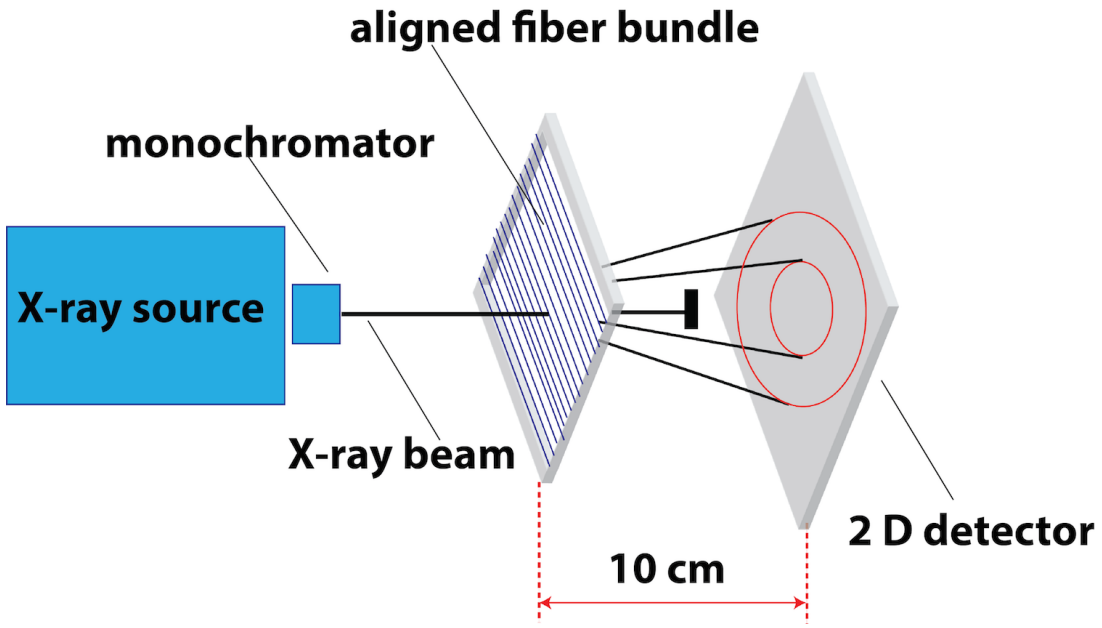

Fig. S5 Illustration of Transmission WAXS geometry. The fibers were aligned horizontally into a bundle and placed perpendicularly into a monochromatic x-ray beam. The scattering patterns were collected by a CCD detector at a distance of 10 cm away from sample.

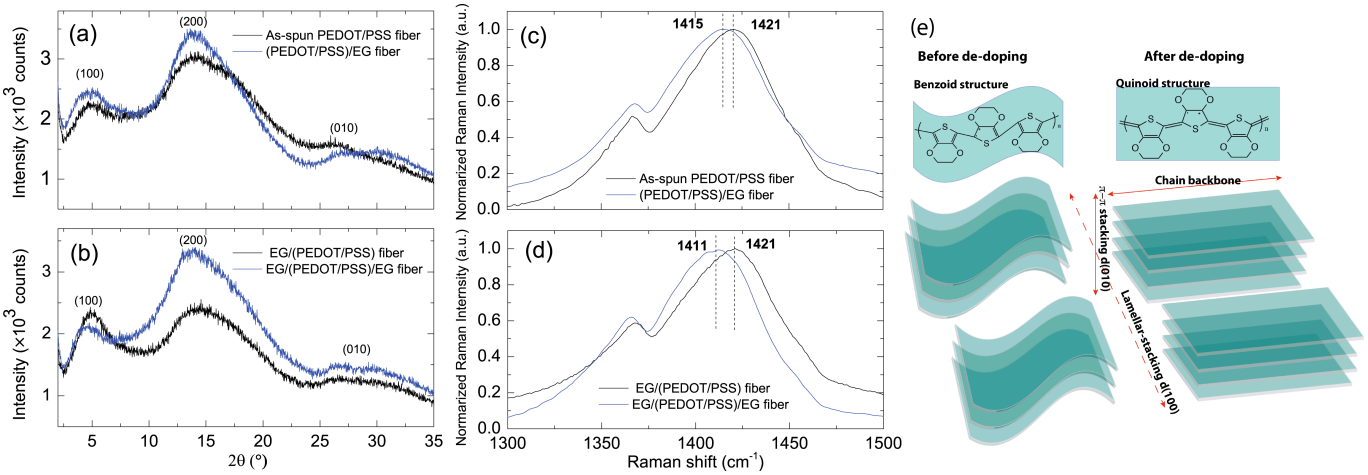

Fig. S6 Microstructure of the conductive polymer microfibers. (a), (b) Wide-angle X-ray diffraction of the conductive polymer fibers. (c) and (d) Raman spectra of the conductive polymer fibers. (e) A schematic of the microstructure change of PEDOT chains before and after EG de-doping.

To understand the electrical transport in the fibers, microstructure characterization of the fibers was carried out by normal XRD and Raman spectroscopy. Fig. S6a and b present the XRD patterns of PEDOT/PSS fibers with or without EG doping and/or de-doping. For the as-spun PEDOT/PSS fiber, the XRD patterns

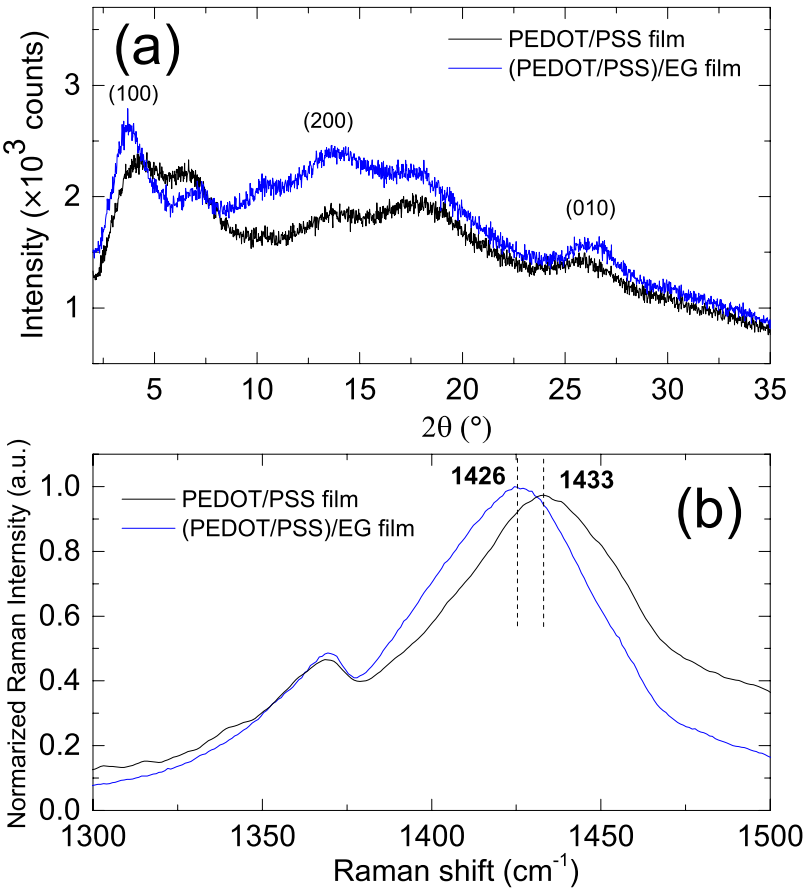

Fig. S7 (a) Wide-angle X-ray diffraction pattern of PEDOT/PSS film and EG de-doped PEDOT/PSS film. (b) Raman spectra of PEDOT/PSS film and EG de-doped PEDOT/PSS film.

show four characteristic peaks at 2θ values of 4.7 °, 14.0°, 17.5° and 26.3° that correspond to lattice spacings (d) of 18.7, 6.3, 5.1 and 3.4 Å, respectively as calculated using Brag's Law.[9] Three peaks of interest at 2θ = 4.7, 14.0 and 26.3 ° correspond to the lamella stacking distance, $d_{(100)}$, of alternate orderings of PEDOT and PSS in the plane, its second-order reflection with the stack distance, $d_{(200)}$, and the interchain planar $\pi-\pi$ stacking distance $d_{(010)}$ of PEDOT, respectively.[10,11] In fact, the as-spun fiber has the same $\pi-\pi$ stacking distance as the EG de-doped PEDOT/PSS films ($d_{(010)}$= 3.4 Å),and the EG de-doped Clevios P and Clevios PH500 fibers ($d_{(010)}$= 3.4 Å)[8], which indicates that wets-pinning of the fibers incorporating hot-drawing prompts aligment of the molecular chains, thus reducing the $\pi-\pi$ stacking distance of the PEDOT chains from 3.5 to 3.4 Å. After de-doping these as-spun fibers with EG, one of the high-angle peaks at 2θ = 17.7° indicating amorphous halo of PSS chains almost disappeared, while the intensity of second-order lamella stacking at 2θ = 14° increased noticeably. This change can be attributed to the partial removal of amorphous PSS in these fibers by EG de-doping. Another peak representing the interchain planar $\pi-\pi$ stacking distance, $d_{(010)}$, of PEDOT, became broader and centered at 2θ = 27° (corresponding to the lattice spacing $d_{(010)}$ = 3.3 Å). It is necessary to note the lack of a distinct shift in the characteristic peak of lamella stacking at 2θ = 4.7° after de-doping of as-spun fibers (Fig. S6a), indicating no obvious planarization of

alternating PEDOT and PSS polymer chains. By incorporating both doping and de-doping of EG, the $d_{(100)}$ peak shifted from 4.7 to 4.1°. The $d_{(010)}$ peak shifted from 26.3 to 28.0°, corresponding to a further reduction of $\pi-\pi$ stacking distance from 3.4 to 3.2 Å. It is important to note that the intensity of the $d_{(010)}$ peak obviously increased after EG de-doping, suggesting that the crystallinity had increased in the fibers. The corresponding lattice distance and percentage of crystalinity for all samples are listed in Table S1. Fig. S6a, b and Table S1 indicate that the most effective way to increase the order of the molecular chains and percentage of crystalinity of the fibers involves partially stretching the molecular chains by hot-drawing, planarization of the thiophene rings on PEDOT by EG doping and reduction of the $\pi-\pi$ stacking distance of PEDOT chains by EG de-doping.

Fig. S6c and d show the Raman spectra of PEDOT/PSS fibers. The strong peak at 1421 cm^{-1} is assigned to the $C_\alpha = C_\beta$ symmetric stretching of the thiophene ring in PEDOT chains in as-spun PEDOT/PSS fibers .[5,12] Note that the position of the peak is 16 cm^{-1} lower than pristine PEDOT/PSS films (Fig. S7b) and 5 cm^{-1} lower than other PEDOT/PSS fibers. This suggests that the quinoid structure of the thiophene rings dominate in our conductive PEDOT/PSS fibers (368 S cm^{-1}) over benzoid structures. This peak did not show an obvious shift after doping with 3 wt% EG. However, after de-doping the as-spun PEDOT/PSS fiber and the EG/(PEDOT/PSS) fiber, the peak shifted from 1421 to 1415 and 1411 cm^{-1}, respectively. The peak shift to 1411 cm^{-1} indicated the most preferred quinoid structure and resulted in the record conductivity of 2804±311 S cm^{-1}. Fig. S6e shows a schematic microstructure of the change of the fibers before and after de-doping as manifested by XRD and Raman results. Though it is beyond the scope of this study to quantify the ratio between the quinoid and benzoid structures in the fibers, we could still remark that a more favorable quinoid structure in the fiber leads to planarization of the conductive PEDOT chains, resulting in the reduction of $\pi-\pi$ stacking distance. As a result, the electrical transport in the most conductive fibers becomes three-dimensional, because the electrons diffuse to a neighboring chain prior to traveling between defects on a single chain.[13] This reduces the electron path-ways on the chains and results in high conductivity of the fibers.

Table S2 2θ and d-spacing values of different PEDOT/PSS fibers and films extracted from Fig. S6 and Fig. S7.

Sample	$2\theta(^\circ)/d_{(100)}$(Å)	$2\theta(^\circ)/d_{(200)}$(Å)	$2\theta(^\circ)/d_{(010)}$(Å)	Crystallity
As-spun PEDOT/PSS fibers	4.71/18.70	14.00/6.30	26.33/3.38	27.8%
EG/(PEDOT/PSS) fibers	4.73/18.60	14.22/6.21	26.32/3.38	27.4%
(PEDOT/PSS)/EG fibers	4.47/19.75	13.7/6.45	27.00/3.30	38.2%
EG/(PEDOT/PSS)/EG fibers	4.20/22.30	13.60/6.50	27.02/3.30	39.8%
PEDOT/PSS film	4.22/20.88	13.73/6.45	25.74/3.46	11.0%
(PEDOT/PSS)/EG film	3.64/24.25	13.73/6.44	26.36/3.38	19.0%

4 Mechanical property evaluation

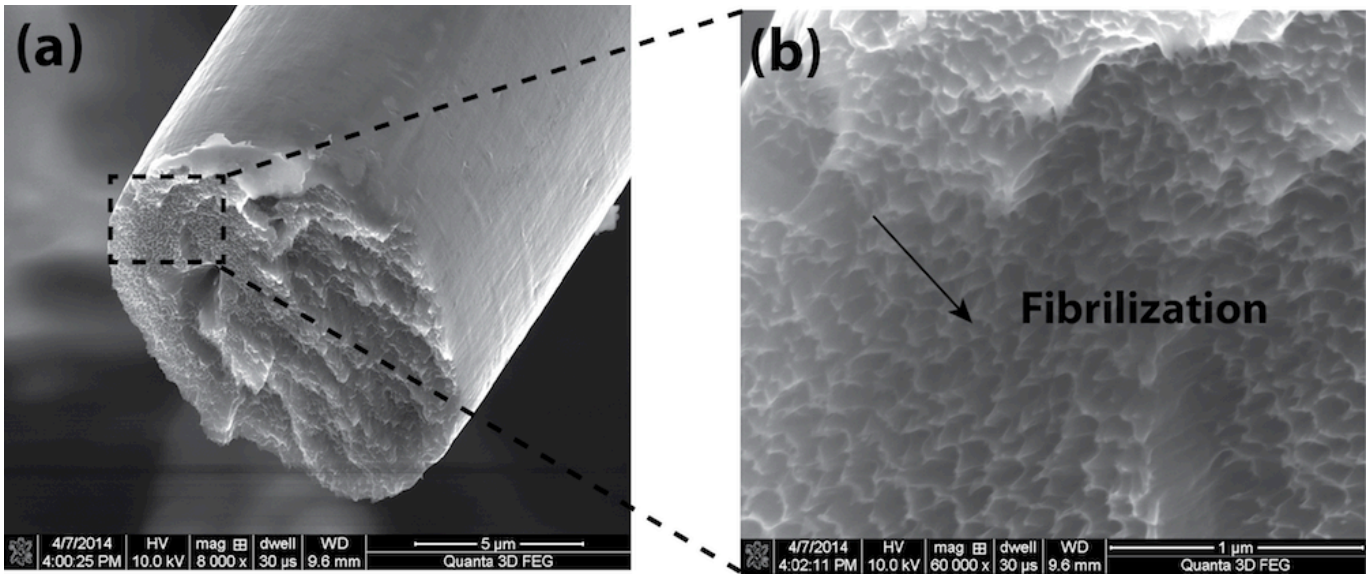

Fig. S8 SEM images of as-spun PEDOT/PSS fibers after tensile testing show that fibrils are protruding from the cross-sections.

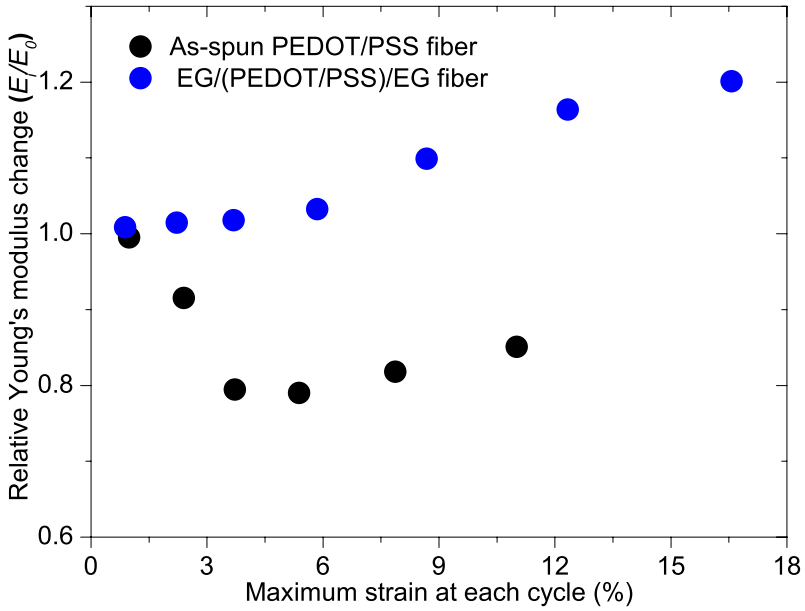

Fig. S9 Relative changes in the Young's modulus of the as-spun PEDOT/PSS fiber and EG/(PEDOT/PSS)/EG fiber at maximum strain of each cycle.

References

1 K. S. Hwang, C. A. Lin and C. H. Lin, *Journal of Applied Polymer Science*, 1994, **52**, 1181–1189.
2 H. Fujiwara, M. Shibayama, J. H. Chen and S. Nomura, *Journal of Applied Polymer Science*, 1989, **37**, year.
3 Y. Xia and J. Ouyang, *ACS Appl Mater Interfaces*, 2012, **4**, 4131–4140.
4 D. Alemu, H. Wei, K. Ho and C. Chu, *Energ Environ Sci*, 2012, **5**, 9662–9671.
5 R. Jalili, J. M. Razal, P. C. Innis and G. G. Wallace, *Advanced Functional Materials*, 2011, **21**, 3363–3370.
6 R. Jalili, J. M. Razal and G. G. Wallace, *Journal of Materials Chemistry*, 2012, **22**, 25174–25182.
7 H. Okuzaki and M. Ishihara, *Macromolecular Rapid Communications*, 2003, **24**, 261–264.
8 H. Okuzaki, Y. Harashina and H. Yan, *European Polymer Journal*, 2009, **45**, 256–261.
9 R. Guinebretiere, in *Kinematic and Geometric Theories of X-ray Diffraction*, ISTE, London and Newport Beach, 1st edn, 2007, pp. 24–26.
10 N. Kim, B. H. Lee, D. Choi, G. Kim, H. Kim, J. R. Kim, J. Lee, Y. H. Kahng and K. Lee, *Physical Review Letters*, 2012, **109**, year.
11 N. Kim, S. Kee, S. Lee, B. Lee, Y. Kahng, , Y. Jo, B. Kim and K. Lee, *Adv Mater*, 2014, **26**, 2268–2272.
12 J. Zhou and G. Lubineau, *ACS Appl Mater Interfaces*, 2013, **5**, 6189–6200.
13 A. Heeger, N. Sariciftci and E. Namdas, in *Metallic State of Conducting Polymers*, Oxford University Press, Oxford, New York, 1st edn, 2010, pp. 1–278.